



TECHNICAL UNIVERSITY OF CLUJ-NAPOCA

ACTA TECHNICA NAPOCENSIS

Series: Applied Mathematics, Mechanics, and Engineering  
Vol. 59, Issue I, March, 2016

## NUMERICAL SIMULATION OF THE FINE BLANKING PROCESS

Nicolae MIHĂILESC, Horațiu IANĂU, Gheorghe ACHIMAȘ

**Abstract:** *The following technologies can be used to obtain high-precision metallic parts made of sheet metals: classic stamping followed by strengthening and finishing through stamping; blanking and piercing with special tools operated by presses; precision blanking and piercing with special tools and machining. Precision stamping with special tools and machining belong to the series and mass production for obtaining parts with high dimensional accuracy, and the surfaces resulting through separation have a quality comparable with that met in grinding. The success of fine stamping operations mainly depends on controlling some parameters such as the clearance between the punch and the cutting die, respectively the pressure level applied by the clamping ring and the counter-punch. Achieving detailed information about the mechanics of the deformation and separation process applied to the semi-finished product allows eliminating the risk of rejection appearance. Using simulation programs is justified exactly through this challenge. Nowadays, the finite element method is widely used in computer-aided design of cold pressing technologies. For the numeric simulation of precision stamping process the program Abaqus/Explicit was adopted.*

**Key words:** *fine blanking, finite element method, Abaqus/Explicit.*

### 1. INTRODUCTION

The fine blanking process takes place in conditions different from those met in classical stamping. The difference consists in:

- Assuring a much lower separation speed, favorable to the shearing process ( $v \approx 15$  mm/s)
- Creating a complex stress state of the material intended for stamping, in the separation area
- Executing the separation with dies that have the clearance between the active elements much lower than in classical stamping ( $j=0$ ;  $j < 0$ )

For the numerical simulation of fine stamping process the program Abaqus/Explicit [5], [6],[7] was adopted. Among the advantages of using this program, the most important are:

- Existence of a graphical pre-processor, through which the finite element model of a pressing process can be easily generated
- Import facilities of some geometric models in various recognized formats of

CAD programs (for example IGES, STEP, DXF, etc.)

- Flexibility concerning the description of the process that represents the subject of the analysis due to "in steps" decomposition mechanism
- Existence of fracture criteria adequate to analyzing the processes dominated by shearing stress
- Existence of a finite element library which is extremely rich
- Existence of a module that is specialized for the automatic meshing of the blank and tools.

If in classical stamping no special conditions are applied, regarding the processed material, in fine blanking it is necessary to use adequate materials for these types of processing. The conditions regarding the material intended for stamping are compulsory, especially in pre-stress stamping applied on the separation area [3]. For accurate blanking, the following conditions are imposed for the material [2], [8]:

- Physical-mechanical properties properly chosen for this type of processing
- Isotropy of mechanical properties
- Minimum metal sheet thickness tolerances.

Materials with low tensile strength, low yield stress and high elongation have a good workability through fine blanking.

## 2. DEFINING THE PARAMETERS OF THE FINE BLANKING PROCESS

The blank behavior is described using an elastoplastic constitutive model [1]. This model defines the elastic part of the deformation according to Hooke's law, in its structure appearing Young's modulus (E) and Poisson's ratio ( $\nu$ ). For describing the irreversible part of deformation, the model uses a yield criterion [1].

$$\bar{\sigma}(\sigma_x, \sigma_y, \sigma_z, \tau_{xy}, \tau_{yz}, \tau_{zx}) = Y[\bar{\epsilon}^{(p)}]. \quad (1)$$

Its expression involves the equivalent stress von Mises,

$$\bar{\sigma}(\sigma_x, \sigma_y, \sigma_z, \tau_{xy}, \tau_{yz}, \tau_{zx}) = \left\{ \frac{1}{2} [(\sigma_x - \sigma_y)^2 + (\sigma_y - \sigma_z)^2 + (\sigma_z - \sigma_x)^2] + 3(\tau_{xy}^2 + \tau_{yz}^2 + \tau_{zx}^2) \right\}^{1/2} \quad (2)$$

(defined as function of the stress components  $\sigma_x, \sigma_y, \sigma_z, \tau_{xy}, \tau_{yz}$  and  $\tau_{zx}$ ), respectively a hardening law that defines the current yield stress Y of the material as dependent on the state parameter  $\bar{\epsilon}^{(p)}$  (the so-called equivalent plastic strain)

$$Y[\bar{\epsilon}^{(p)}] = \begin{cases} Y_{p0.2} + (Y_g - Y_{p0.2}) \frac{\bar{\epsilon}^{(p)}}{\bar{\epsilon}_g^{(p)}}, & \text{if } 0 \leq \bar{\epsilon}^{(p)} \leq \bar{\epsilon}_g^{(p)}, \\ Y_g, & \text{if } \bar{\epsilon}^{(p)} > \bar{\epsilon}_g^{(p)}. \end{cases} \quad (3)$$

In equations (3) the following material parameters appear, determined through uniaxial tensile tests:

- Equivalent plastic strain associated to the uniform elongation  $A_g$  [%],

$$\bar{\epsilon}_g^{(p)} = \ln \left( 1 + \frac{A_g}{100} \right) \quad (4)$$

- Yield stress associated to the yield strength  $R_{p0.2}$  [N/mm<sup>2</sup>],

$$Y_{p0.2} = R_{p0.2} \left( 1 + \frac{0.2}{100} \right) = 1.002 \cdot R_{p0.2}, \quad (5)$$

- Ultimate tensile stress associated to the uniform elongation  $A_g$  [%] and the ultimate tensile strength  $R_m$  [N/mm<sup>2</sup>],

$$Y_g = R_m \left( 1 + \frac{A_g}{100} \right) \quad (6)$$

Table 1 presents the input data used for calibrating the constitutive model of the M50 sheet metal with the thickness of 2.5 mm.

Table 1

**Parameters that define the elasto-plastic constitutive model for M50 sheet metal with a nominal thickness of 2.5 mm.**

Mass density	$\rho$	$7,85 \cdot 10^{-6}$ kg/mm <sup>3</sup>
Elastic constant	E	$2,1 \cdot 10^5$ N/mm <sup>2</sup>
	$\nu$	0,3
Parameters that define the hardening law	$A_g$	11%
	$R_{p0.2}$	500 N/mm <sup>2</sup>
	$R_m$	948 N/mm <sup>2</sup>

The fracture of the blank is detected using a criterion based on the critic level of equivalent plastic strain [5]

$$D = \frac{1}{\bar{\epsilon}_{crit}^{(p)}} \int d\bar{\epsilon}^{(p)} \quad (7)$$

where  $\bar{\epsilon}_{crit}^{(p)}$  represents a material constant. Practically,

$$D < 1 \quad (8)$$

corresponds to plastic strain levels that do not cause the fracture, while

$$D \geq 1 \quad (9)$$

individualizes the fracture states. Confronting the experimental data with the numeric simulations highlights that, for M50 sheet metal with a nominal thickness of 2.5 mm, the best results are obtained for

$$\bar{\epsilon}_{crit}^{(p)} = 1. \quad (10)$$

The numerical simulation presented in this paper was made in the following conditions (see Fig. 1):

- The nature of the analyzed process: fine blanking of a circular part

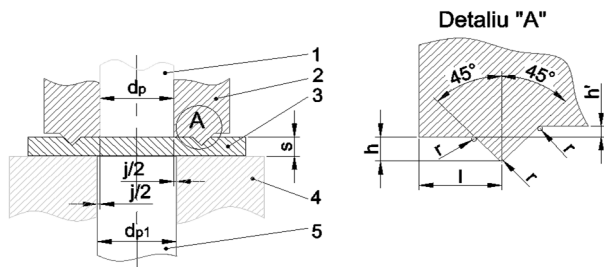


**Fig. 1.** Fine blanking principle: 1-punch, 2-clamping ring, 3-blank, 4- die, 5-counter-punch

- Blank material: M50 metallic sheet with a thickness of

$$s = 2.5 \text{ mm} \quad (11)$$

- Diameter of the finished part

$$D = 40 \text{ mm} \quad (12)$$

- Optimal value of the clearance between the punch and the blanking die – truncated at a 0.01 mm [3]

$$j = 0.01 \cdot s = 0.01 \cdot 2.5 = 0.025 \text{ mm} \rightarrow j = 0.02 \text{ mm} \quad (13)$$

- Diameter of the blanking die [3]

$$d_{pl} = D = 40 \text{ mm} \quad (14)$$

- Punch diameter [3]

$$d_p = d_{pl} - j = 40 - 0.02 = 39.98 \text{ mm} \quad (15)$$

- Dimensional parameters of the rib located on the surface of the clamping ring – see the detail in Figure 1 [3]

$$\begin{aligned} \ell &= 1.7 \text{ mm} \\ h &= 0.5 \text{ mm} \\ r &= 0.2 \text{ mm} \\ h' &= 0.1 \text{ mm.} \end{aligned} \quad (16)$$

- Stamping force acting on the rib rounded to multiple of 10000 N [3]

$$Q_1 = \pi(d_p + 2\ell)q_1 = 156724,6 \text{ N} \rightarrow Q_1 = 160000 \text{ N}, \quad (17)$$

where  $q_1 = 1150 \text{ N/m}$  [3] is the specific pressure force

- Force applied by the counter-punch rounded to multiple of 10000 N [3]

$$Q_2 = \frac{\pi d_{pl}^2}{4} q_2 = 87964,6 \text{ N} \rightarrow Q_2 = 90000 \text{ N}, \quad (18)$$

where  $q_2 = 70 \text{ N/mm}^2$  is the counter pressure (case of blanking without calibrating the planar surfaces)

- Punch stroke [3]:

$$H = 1.2 \cdot s = 1.2 \cdot 2.5 = 3 \text{ mm}. \quad (19)$$

In what follows, the main steps of the finite-element model preparation, as well as the interpretation of the numerical results will be presented.

### 3. FINITE-ELEMENT SIMULATION OF THE FINE BLANKING PROCESS USING ABAQUS/EXPLICIT

The computational scheme used by the Abaqus/Explicit finite-element program is of dynamic type [5]. For this reason, a complete description of the material behavior involves:

- Defining the mass density
- Defining the elastic characteristics of the blank
- Defining the hardening law of the blank
- Defining the tangential component of frictional contact interactions
- Defining the geometry of the blank.

Defining the kinematic constraints and loads that act during the fine blanking process:

- For the blank: the kinematic constraints apply at the level of nodal degrees of freedom.
- The blanking, being a fixed component, has its reference point fully clamped.
- For the punch, counter-punch and clamping ring only vertical motions are allowed.
- In the case of the punch, the vertical displacement is defined through the diagram shown in Figure 2 (see also equation (19))
- The counter-punch and clamping ring receive vertical forces defined through equations (17) and (18). These forces evolve according to the diagram shown in Figure 3.

The finite-element model of the fine blanking process was defined using the graphical pre-

processor Abaqus/CAE [6]. The steps of elaborating this model were the following ones:

- Importing the geometric models of the blank and tools.

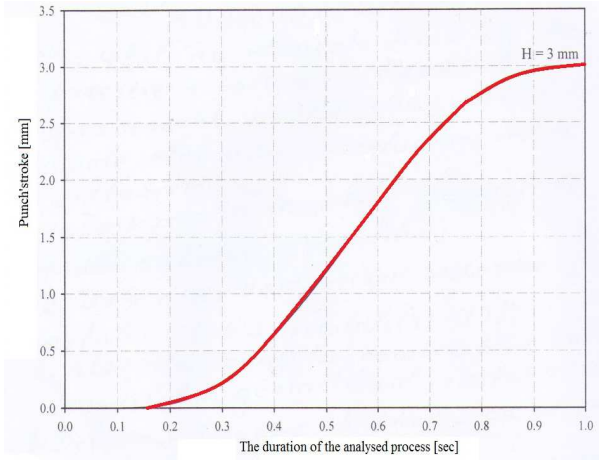


**Fig. 2.** Curve describing the vertical displacement of the punch on a distance of 3 mm.

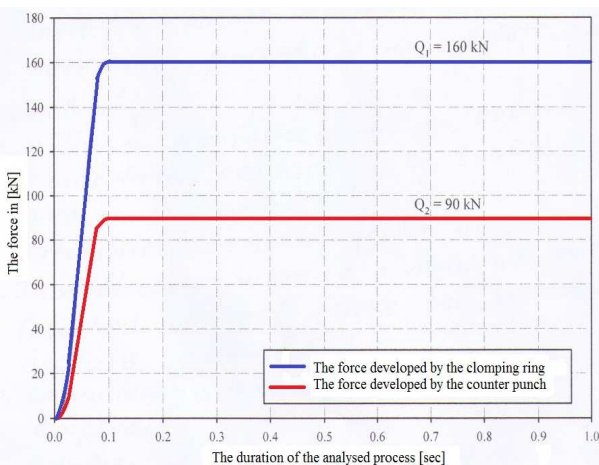


**Fig. 3.** Curves describing the evolution of the forces developed by the clamping ring and counter-punch.

- Describing the mechanical behavior of the blank (see Table 1 and equations (3)-(6))
- Attaching the constitutive equations to the geometric model of the blank
- Defining the fine blanking process as an analysis step
- Defining the parameters describing the contact interactions between the blank and tools
- Defining the blank as an entity that can form contact with itself during the analyzed process
- Specifying the kinematical constraints

- Automatic meshing of the blank using finite elements with axial symmetry CAX4R [5] – see Figure 4
- Running the Abaqus/Explicit solver
- Analysis and interpretation of the numerical results.

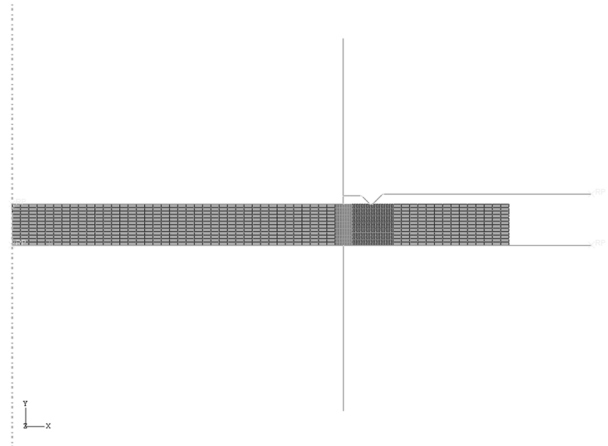


**Fig. 4.** Automatic meshing of the blank using finite elements with axial symmetry CAX4R.

Among the information provided by the Abaqus/Viewer postprocessor [7], the following aspects are of high importance for the fine blanking simulation:

- Distribution of equivalent plastic strain in the axial section of the blank (see Figures 5 and 6)
- Variation of the force developed by the punch depending on its stroke (Figure 7)

As a state parameter, the equivalent plastic strain defines the level of hardening accumulated by the material during the fine blanking process. As one may notice in Figures 5 and 6, the hardening is mostly concentrated in two regions of the blank: shearing area and the region placed in the neighborhood of the rib. The largest value of the equivalent plastic strain (0.90) is located under the rib. Some portions of the shearing area also have levels of the equivalent plastic strain close to the maximum value. When interpreting the diagrams shown in Figures 5 and 6, the following aspect must be taken into account: these diagrams do not contain information related to the finite elements previously removed from the mesh due to fracture. At the level of these elements, the equivalent plastic strain accumulated during the blanking process has already reached the critical level  $\bar{\epsilon}_{crit}^{(p)} = 1$  (see equation (10)).

The diagrams presented in Figures 5 and 6 do not show the existence of any burrs in the shearing area. This situation is a consequence of the small clearance between the punch and blanking die combined with the pressure exerted by the counter-punch and clamping ring during the fine blanking process.

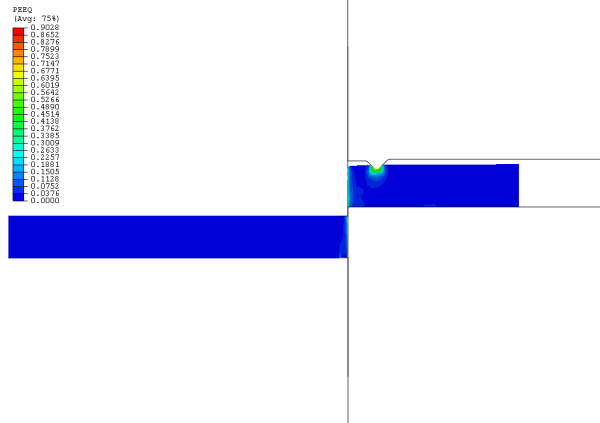


**Fig. 5.** Distribution of the equivalent plastic strain in the axial section of the blank (final stage of the fine blanking process).

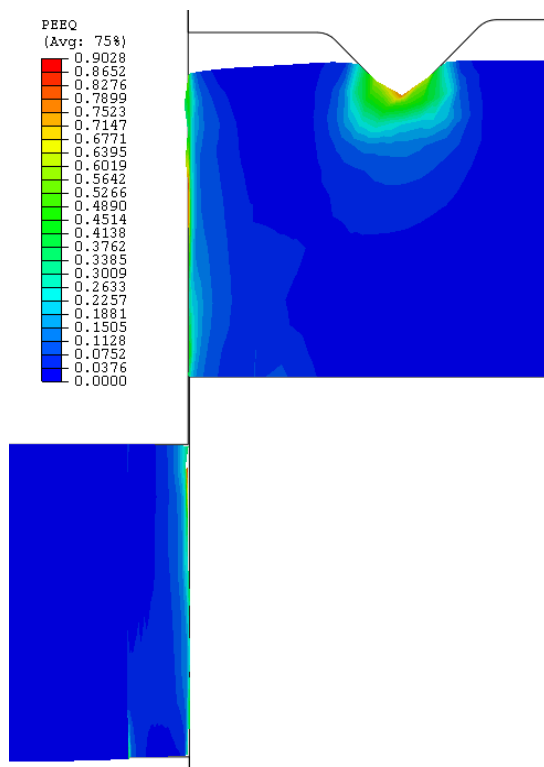


**Fig. 6.** Distribution of the equivalent plastic strain in the axial section of the blank (final stage of the fine blanking process; detail referring to the shearing zone).

The diagram shown in Figure 7 describes a force evolving in the manner specific to blanking process:

- Aggressive increase up to a maximum level (230.9 kN) at which the fracture begins
- Quick decrease to a quasi-stable level (93 kN) that compensates the force exerted by the counter-punch and the friction between blank and tools.

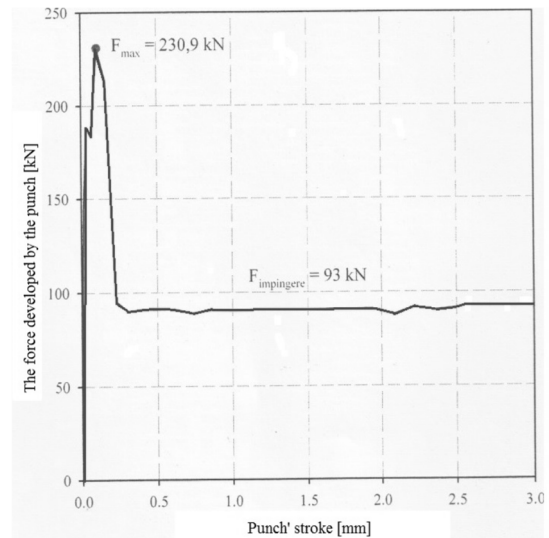


**Fig. 7.** Evolution of the force developed by punch during the fine blanking process.

#### 4. CONCLUSIONS

Following the numerical simulation of the fine blanking process, the following conclusions can be formulated:

- The distribution domain of the surface dimensions of the finished parts is considerably narrower than in the case of parts obtained by classical blanking procedures. This characteristic, along with the quality of the shearing surfaces and the lack of burr represents the main advantage of the fine blanking.
- The improved dimensional accuracy of the parts obtained by fine blanking procedures can be also justified if the reduced value of the clearance between the punch and die is taken into account.
- The pressure exerted by the clamping ring and counter-punch also has a beneficial effect on the accuracy and quality of the shearing zone. In general, the pressure allows a better filling of the gap between punch and die and also increases the hardening accumulated by the sheet metal. Under such circumstances, the

elastic springback after their removal from the die will be also considerably diminished.

- The disappearance of the burr is a consequence of the reduced clearance combined with the pressure exerted by the clamping ring and punch.

## 5. REFERENCES

- [1] Chakrabarty, J. *Applied Plasticity*, Springer Publishing House, New York, 2010.
- [2] Iliescu, C. et al. *Tehnologia debitării decupării și perforării de precizie*, Editura Tehnică, București, 1980.
- [3] Mihai, N.M. *Cercetări privind prelucrabilitatea tablelor prin ștanțare de precizie. Teză de doctorat*, U.T. Cluj-Napoca, 2008.
- [4] Suchy, I. *Handbook of Die Design*, McGraw-Hill Publishing House, New York, 2006.
- [5] \*\*\* *Abaqus Analysis User's Manual. Version 6.9-3*, Abaqus, Inc., Providence, 2009.
- [6] \*\*\* *Abaqus/CAE User's Manual. Version 6.9-3*, Abaqus, Inc., Providence, 2009.
- [7] \*\*\* *Abaqus/Viewer User's Manual. Version 6.9-3*, Abaqus, Inc., Providence, 2009.
- [8] \*\*\* *Fine-Blanking Practical Handbook*, Feintool AG, Lyss, 1972.

## SIMULAREA NUMERICĂ A PROCESULUI DE ȘTANȚARE FINĂ

**Rezumat:** Pentru obținerea pieselor metalice cu precizie ridicată din tablă se pot folosi următoarele tehnologii: ștanțarea clasică, urmată de îndreptare și de finisare tot prin ștanțare, pe contur, decupare și perforare cu scule speciale, acționate de prese, decupare și perforare de precizie cu scule și mașini speciale. Ștanțarea de precizie cu scule și mașini speciale se aplică în producția de serie și de masă, pentru obținerea unor piese având o înaltă precizie dimensională, iar suprafețele ce rezultă prin separare au un grad de netezime comparabil cu cel de la rectificare. Succesul operațiilor de ștanțare fină depinde în principal de controlul unor parametri precum jocul dintre poanson și placa de tăiere, respective nivelul presiunii exercitate de inelul de strângere și contra-poanson. Dobândirea unor informații detaliate și rupere a semifabricatului permite eliminarea riscului de apariție a rebuturilor. Utilizarea programelor de simulare se justifică tocmai prin acest deziderat. În prezent, metoda elementelor finite este folosită pe scară largă în domeniul proiectării asistate de calculator a tehnologiilor de presare la rece. Pentru simularea numerică a procesului de ștanțare de precizie a fost adoptat programul Abaqus/Explicit.

**Nicolae MIHĂILESC**, PhD Student, Eng., Technical University of Cluj-Napoca, Department of Manufacturing Engineering, 103-105 Muncii Blvd. 400641 Cluj-Napoca, Office Phone: 0040 264 401731

**Horațiu IANCĂU**, Prof. PhD. Eng., Technical University of Cluj-Napoca, Department of Manufacturing Engineering, 103-105 Muncii Blvd. 400641 Cluj-Napoca, Office Phone: 0040 264 401731

**Gheorghe ACHIMAȘ**, Prof. PhD. Eng., Technical University of Cluj-Napoca, Department of Manufacturing Engineering, 103-105 Muncii Blvd. 400641 Cluj-Napoca, Office Phone: 0040 264 401731